Development 136, 95-105 (2009) doi:10.1242/dev.027698

# The actin-binding protein Lasp promotes Oskar accumulation at the posterior pole of the *Drosophila* embryo

**Ritsuko Suyama*, Andreas Jenny*,†, Silvia Curado*,‡, Wendy Pellis-van Berkel§ and Anne Ephrussi¶**

During *Drosophila* oogenesis, *oskar* mRNA is transported to the posterior pole of the oocyte, where it is locally translated and induces germ-plasm assembly. Oskar protein recruits all of the components necessary for the establishment of posterior embryonic structures and of the germline. Tight localization of Oskar is essential, as its ectopic expression causes severe patterning defects. Here, we show that the *Drosophila* homolog of mammalian Lasp1 protein, an actin-binding protein previously implicated in cell migration in vertebrate cell culture, contributes to the accumulation of Oskar protein at the posterior pole of the embryo. The reduced number of primordial germ cells in embryos derived from *lasp* mutant females can be rescued only with a form of Lasp that is capable of interacting with Oskar, revealing the physiological importance of the Lasp-Oskar interaction.

**KEY WORDS: Lasp, Oskar, Actin cytoskeleton, *Drosophila***

## INTRODUCTION

In *Drosophila melanogaster*, maternally provided mRNAs and proteins are transported from the nurse cells into the growing oocyte and stored until they are required at later stages of development. *oskar* mRNA, which encodes the posterior determinant of the fly, is transported to the posterior pole of the oocyte, where it is localized from stage 8 of oogenesis onward (Ephrussi et al., 1991; Kim-Ha et al., 1991). *oskar* mRNA is exclusively translated after its localization (Kim-Ha et al., 1995; Markussen et al., 1995; Rongo et al., 1995), and thus locally induces the assembly of the pole-plasm, the germ-plasm of *Drosophila*, causing abdomen and germline formation in the embryo. Oskar protein is both necessary and sufficient for abdomen induction and germline formation (Ephrussi and Lehmann, 1992). Mislocalization of *oskar* mRNA to the anterior, as occurs in *BicD* mutants (Ephrussi et al., 1991), or ectopic expression of Oskar at the anterior pole from an *oskar-bicoid* (*osk-bcd*) transgene (Ephrussi and Lehmann, 1992), causes strong embryonic patterning defects and, in the latter case, the formation of primordial germ cells at the anterior of the embryo. It is therefore essential that Oskar activity remains restricted to the posterior pole of the oocyte and embryo.

*oskar* mRNA and protein remain tightly associated with the posterior pole during oogenesis and early embryogenesis, in spite of the strong cytoplasmic streaming that occurs after stage 10B of oogenesis (Gutzeit and Koppa, 1982), and experiments with the actin-severing drugs Cytochalasin D and Latrunculin A suggest that *oskar* mRNA and protein are attached to the actin cytoskeleton (Lantz et al., 1999). In addition, and in contrast to Oskar, Bicoid protein diffuses along the anteroposterior axis after its synthesis and is detected down to 30% of the egg length, although its mRNA is restricted to the anterior pole in the embryo [100-80% egg length (Driever and Nusslein-Volhard, 1988)], which suggests that mRNA localization is not sufficient for protein restriction. Posterior anchoring of Oskar requires the Oskar protein itself (Ephrussi et al., 1991; Kim-Ha et al., 1991), and is a dynamic process involving both actin-dependent and -independent processes (Babu et al., 2004; Tanaka and Nakamura, 2008; Vanzo et al., 2007). We performed an extensive yeast two-hybrid screen with Short-Oskar (the isoform of Oskar that is required for pole cell formation) as bait, to search for potential anchoring proteins, and found that the *Drosophila* homolog of mammalian Lasp1 (Grunewald and Butt, 2008) binds to Oskar and helps to anchor Oskar to actin at the posterior pole. Furthermore, we found that efficient pole cell formation in vivo requires a Lasp SH3 domain that is capable of interacting with Oskar.

Developmental Biology Unit, European Molecular Biology Laboratory, Meyerhofstrasse 1, D-69117 Heidelberg, Germany.

*These authors contributed equally to this work
†Present address: Department of Developmental and Molecular Biology, Albert Einstein College of Medicine, Chanin 503, 1300 Morris Park Avenue, Bronx, New York, NY 10461, USA
‡Present address: Department of Biochemistry and Biophysics, Genetics, Development and Behavioral Sciences, University of California San Francisco, 1550 Fourth Street, San Francisco, CA 94143, USA
§Present address: Department of Physiological Chemistry, Centre for Biomedical Genetics, UMC Utrecht, Universiteitsweg 100, 3584 CG Utrecht, Netherlands
¶Author for correspondence (e-mail: ephrussi@embl-heidelberg.de)

**Accepted 22 October 2008**

## MATERIALS AND METHODS

### Constructs and transgenes

A detailed description of constructs and transgenes is available on request.

### Two-hybrid screen

The yeast two-hybrid screen was performed using a modified mating strategy (Fromont-Racine et al., 1997). In brief, frozen aliquots of the oligo-dT primed ovarian cDNA library (Grosshans et al., 1999) transformed into the yeast strain EGY48 were mated to RSY473 strains previously transformed with both Short-Oskar fused to NLSLexA at the C terminus and JK103 for 4 hours on YP-Gal plates to simultaneously induce prey protein expression. Cells were washed with medium lacking leucine, tryptophan, uracil and histidine, and plated onto S-Gal/Raf plates lacking leucine, tryptophan, uracil and histidine. Mating efficiencies varied between 2% and 10%. Diploid cells ($3.8\times10^7$) were screened, corresponding to $5.7\times10^6$ primary yeast transformants, and 480 positive clones were analyzed. Table S1 shows a compilation of the screening results (see supplementary material). Eighteen colonies of type 3.30 were further analyzed for this report [3.30 corresponds to bases 2243 to 3240 of the sequence submitted to GenBank (AJ294538)]. Isolated prey plasmids (in pJG4-5) were retransformed into EGY48 and the specificity of the interaction tested by mating to independent bait proteins.

### cDNA cloning, sequencing and Q/RT-PCR

The insert of clone 3.30 was used as a probe to screen an oligo-dT primed ovarian cDNA library in lambda ZAPII kindly provided by A. Spradling and the Berkeley *Drosophila* Genome Project. Several of the longest cDNA

clones were characterized by restriction mapping and end-sequencing. Two clones were chosen for sequencing. Templates were generated using the GPS-1 transposon system (NEB, Madison, WI, USA) and sequenced with fluorescent-labeled primers on an Arakis sequencer (EMBL).

S-Lasp was amplified from EST AT23571 with Oligo3_BglII (CGGCAGATCTATGAATAAAACCT) and Oligo2a_Not (GCGGCCG-CTTATATAACC), and cloned into pCRIITopo (Invitrogen, Carlsbad, CA, USA). RNA extraction from ovaries and embryos was done as described previously (Hachet and Ephrussi, 2004). Expression of S-Lasp was confirmed by One-step RT-PCR (Invitrogen) using primers LASP859U (GAGAACACCAAAATCCAGTCCAAC) and LASP1552L (CTGTGG-TGGCGGCATCTG). The accession numbers of the assembled cDNA sequences are AJ294538 (L-Lasp) and AT23571 (S-Lasp).

The thermoscript RT-PCR System (Invitrogen) was used to synthesize cDNA for quantitative RT-PCR for *oskar* (see Fig. S3 in the supplementary material). Q-PCR reactions were run on an ABI 7000 Real-time PCR system with primers HJ46F (AACAAATCTTGCACCGCTGGGC) and HJ47R (GACTTGGCGTGGTGAGGCCTGA). RpS49 was used for normalization (rp49F, GCTAAGCTGTCGCACAAA; rp49R, TCCGGTGGGCAGC-ATGTG).

### Interaction assays

The expression constructs for Gst-chicken Src, Gst-mouse NSrc and pSGT_HA_SAM68 were kindly provided by G. Superti-Furga (Ce-M-M, Vienna, Austria) (Lock et al., 1996). Gst-fusion proteins were expressed and purified as described, except that protein expression was induced at 30°C (Breitwieser et al., 1996). HA-tagged Short-Oskar and SAM68 were translated in vitro from pβTHShortHA and pSGT_HA_SAM68 using the TNT-coupled transcription translation kit, according to the manufacturer's instructions (Promega, Madison, WI, USA).

For Gst pull-down experiments, 10 μg of the appropriate Gst-fusion protein were incubated with 15 μl pre-equilibrated glutathione-Sepharose beads (Amersham-Pharmacia, Piscataway, NJ, USA) in 500 μl BP [50 mM Tris/HCl (pH 7.5), 150 mM KCl, 1% NP40, 5 mM EGTA, 5 mM EDTA and 1×EDTA free protease inhibitor cocktail (Roche, Basel, Switzerland)] for 30 minutes at 4°C on a rotating arm. The beads were then washed three times with 1 ml BP and incubated with 5 μl of an in vitro translation reaction in a total volume of 500 μl BP for 1 hour at 4°C. The beads were then washed three times with 1 ml BP and resuspended in 20 μl 2×concentrated SDS sample buffer. Samples were then analyzed on a 12% SDS polyacrylamide gel, dried, exposed to Biomax film (Kodak) and quantified on a Molecular Dynamics phosphorimager.

For the Gst pull-down experiments shown in Fig. S1 (see supplementary material), 10 μg of the appropriate Gst-fusion protein were incubated for 50 minutes with ovary extracts (50 ovary pairs per sample) at 4°C and processed as above. Samples were analyzed on a 10% SDS polyacrylamide gel and processed for western blotting.

### Actin-binding assays

The GN protein was expressed as described above, except that 1 mM DTT was added to the dialysis buffer. Actin co-sedimentation assays were performed following the protocol supplied by the manufacturer (Cytoskeleton, Denver, CO) with several modifications: To pre-clear, the protein solutions were centrifuged for 1 hour at 436,000 ***g*** in a TLA 100 rotor in a Beckmann TL100 ultracentrifuge. G-actin (36 μg) was polymerized in the presence of 30 μg GN or control proteins for 30 minutes at room temperature. The samples were then centrifuged at 279,000 ***g*** under the same conditions as above, for 30 minutes. Ten percent of the resulting pellet was then loaded onto a 10% SDS polyacrylamide gel. All assays were run in duplicate.

### Antibody production

To generate an anti-Lasp antibody, the insert of two-hybrid clone 3.30 was cloned as a *Eco*RI(blunt)/*Xho*I fragment into the *Sma*I and *Sal*I sites of pQE31 (Qiagen, Valencia, CA, USA) and expressed as a $His_6$-tagged fusion protein in *E. coli* strain M15[pRep4] (Qiagen). Protein production was induced with IPTG at 1 mM for 4 hours at 37°C and the protein purified under denaturing conditions as indicated by the manufacturer, except that the protein was step-eluted in buffer C containing 250 mM imidazole. Rabbit (#6528 and #6529) injections and bleedings were carried out by Eurogentec (Belgium). Analogously, the N-terminal *Bgl*II/*Pst*I fragment of pSP72_L_Lasp was subcloned, expressed and used for immunization (#7271). To generate the anti-Oskar antibody, the *Eco*RV/*Sph*I fragment of the Blue-osk cDNA (Ephrussi et al., 1991) was cloned into the *Bam*HI(blunt)/*Sph*I site of pQE32 (Qiagen). The $His_6$-tagged fusion protein was expressed and purified as above, except that the culture was grown at 30°C. The antibody was produced in a rabbit (Anix) by EMBL Laboratory Animal Resources.

Whole-mount antibody staining and RNA in situ hybridizations were performed as described previously (Riechmann and Ephrussi, 2004; Riechmann et al., 2002; Tomancak et al., 2000). Anti-Lasp terminal-bleed serum (#6529), rat anti-Vasa and pre-absorbed rat 56 anti-Oskar (Ephrussi et al., 1991) antibodies were used at dilutions of 1:500-1:2000, 1:1000 and 1:2000, respectively. Fluoresceine-conjugated goat anti-rabbit and rhodamine-conjugated goat anti-rat were used at a dilution of 1:500 (in PBT, Amersham). Samples were analyzed on a Zeiss Axiovert 200 or a Leica TCS SP2 confocal microscope and quantified using ImageJ.

The preparation of ovarian extracts and western blotting were performed as described previously (Markussen et al., 1995). Rabbit anti-Oskar and anti-Lasp antibodies (#6528 and #7271) were used at dilutions of 1:2000 and 1:4000, respectively. An anti α-tubulin monoclonal antibody DM 1A (1:2000, Sigma, St Louis, MO, USA) was used for standardization.

### Hobo excision

Directional *hobo*-mediated deletions were generated by remobilizing the Hobo element of the $P\{wHy\}Lasp^{DG14505}$ insertion (kindly provided by W. Gelbart, Harvard University, USA) as described (Huet et al., 2002). After selecting for $y^-$ or $w^-$ chromosomes, 44 deletion events were analyzed for loss of the appropriate P-element flanking sequence, by single fly genomic PCR using primers for pendout (CGACGGGACCACCTTATGTT) and the insertion flanking *lasp* (5′ primer, ATAGCGAGTCGTACCATTACCATC; and 3′ primer, GGAAGACCACAAAGCCAATTTATA). The extent of the Hobo-mediated deletion was then mapped by inverse PCR as described (Huet et al., 2002). Two $y^-/w^+$ deletions were further characterized. $lasp^{v45}$ and $lasp^{v41}$ delete 2859 bp and 3514 bp with respect to the original insertion point of $P\{wHy\}Lasp^{DG14505}$ (nt 16675541 3L; GB accession number AE014296, release 5.7). RT-PCR (not shown) and western analysis demonstrated that neither *lasp* mRNA is present, and that neither the C terminus (Fig. 4D; anti-Lasp Cterm antibody #6528) nor the N terminus (anti-Lasp Nterm #7271; not shown) of Lasp is expressed. $lasp^{v45}$ and $lasp^{v41}$ are thus molecular null alleles.

### Transgenesis

Transgenic fly lines were generated by P element-mediated transformation of a $w^{1118}$ stock and then balanced (Rubin and Spradling, 1982). Several independent lines were assayed for each construct and results with typical lines are shown in this study.

## RESULTS

### Oskar interacts with *Drosophila* Lasp

In a two-hybrid screen using Short-Oskar as bait, we identified CG3849 (Lasp), the *Drosophila* homolog of vertebrate Lasp1 (LIM and SH3 protein 1; see Fig. S1 in the supplementary material; Fig. 4A) (Chew et al., 1998; Grunewald and Butt, 2008; Schreiber et al., 1998), as being a strong interactor. Lasp consists of an N-terminal LIM domain, followed by two nebulin-like repeats (NEB; Fig. 4A), a spacer region and a C-terminal SH3 domain (for a review, see Grunewald and Butt, 2008). NEB repeats were first identified in human nebulin, an actin-binding, structural muscle protein (Labeit and Kolmerer, 1995). SH3 domains are evolutionarily conserved protein-protein interaction domains of about 60 amino acids (Musacchio et al., 1992a), which are frequently present in cytoskeletal proteins and proteins involved in signal transduction. Within the LIM, NEB and SH3 domains, *Drosophila* Lasp is highly similar to vertebrate and *Caenorhabditis elegans* Lasp, whereas the

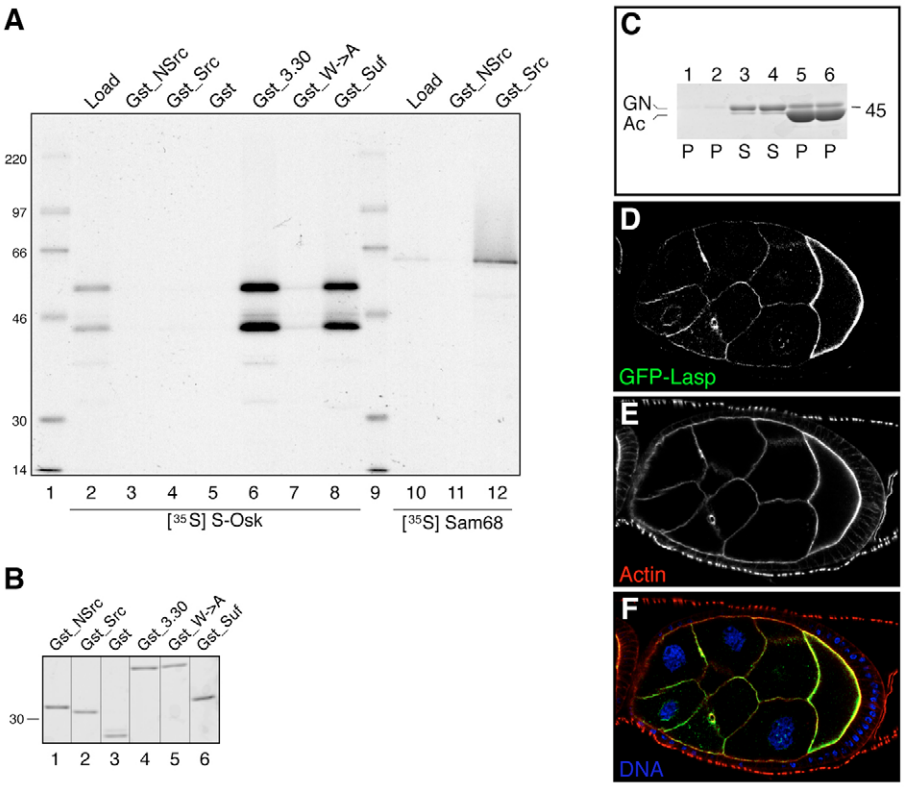


**Fig. 1. Lasp interacts with Oskar in vitro, and binds and colocalizes with actin.** (**A**) Gst pull-down assays show that [$^{35}$S]-labeled Short-Oskar binds to a Gst fusion-protein of the original two-hybrid clone (lane 6, Gst_3.30) and of the SH3 domain of Lasp (lane 8, Gst_Suf). A functional SH3 domain is required for this interaction, as the W→A point mutant version that abolishes physiological SH3 interactions is unable to bind (lane 7, Gst_W→A). Neither Gst fused to the SH3 domain of Src (lane 4), nor Gst alone (lane 5) retains Oskar. However, the Src substrate SAM68 binds to the Src SH3 domain but not to its natural, neuronal, non-binding variant NSrc (lanes 12 and 11, respectively), showing that the SH3 domain of Src is functional. Lanes 2 and 10 contain 10% of the respective labeled proteins added to the binding reactions. The apparent molecular masses of the standards (lanes 1 and 9) are indicated in kDa. (**B**) Coomassie-stained gel showing that comparable amounts of the indicated fusion protein were bound to the glutathione-Sepharose beads. (**C**) Lasp binds to filamentous actin in vitro. The N terminus of Lasp, including the two NEB repeats fused to Gst (GN) co-sediments with F-actin (Ac) in pelletting assays (P, pellets) of duplicate reactions in lanes 5 and 6, supernatants (S) in lanes 3 and 4). Lanes 1 and 2 show that hardly any fusion protein is pelletted in the absence of actin. The position of the 45-kDa molecular mass marker is indicated on the right. (**D-F**) *nanos*-Gal4 driven, germline-specific expression of GFP-tagged full-length Lasp in a stage 8 egg chamber. Lasp (D) and actin (rhodamine phalloidin; E) colocalize around the oocyte cortex, at the nurse cell borders and on ring canals (F). DNA is stained in blue (DAPI).

spacer between the NEB repeats and the SH3 domain is not conserved, and its length varies greatly between different species (see Fig. S1E in the supplementary material).

More detailed analysis showed that both the Short- and Long-Oskar isoforms interact with Lasp and that the interaction is specific for the SH3 domain of Lasp (see Fig. S1A-C in the supplementary material). Furthermore, GST fused to the original two-hybrid fragment of Lasp (3.30) or to the SH3 domain only were able to precipitate [$^{35}$S]-labeled, in vitro-translated Short-Oskar (Fig. 1A). However, as quantified by phosphorimager analysis, a mutant Lasp SH3 domain, in which a tryptophan that is strictly required for physiological SH3 interactions (Musacchio et al., 1992b; Musacchio et al., 1994) was changed to alanine (Gst_W→A), was at least 15-fold less efficient in precipitating Short-Oskar, confirming that the Lasp-Oskar interaction behaves as expected for a canonical SH3 domain interaction (Fig. 1A). Neither equal amounts (Fig. 1B) of Gst alone, nor Gst fused to the SH3 domain of Src (Gst_Src) or to the neuronal variant of the Src SH3 domain (Gst_NSrc) was capable of binding Short-Oskar (Fig. 1B). GST-pull downs of Oskar from ovary extracts showed similar results (see Fig. S1D in the supplementary material). Thus, independent assay systems show that Oskar and Lasp interact specifically.

## Lasp and Oskar localization overlaps in oocytes and embryos

For the interaction of Lasp with Oskar to be physiologically relevant, the distribution of the two proteins should overlap in vivo. Consistent with in situ hybridization data (not shown), antibodies against the initial two-hybrid fragment of Lasp strongly stain region 2 and two or so cells at the anterior tip of the germarium (Fig. 2A). Double-labeling experiments showed that these cells do not express Hts, which suggests that they are cap cells rather than germline stem cells (data not shown) (Lin et al., 1994). During mid-oogenesis, Lasp is strongly expressed in nurse cells and is highly enriched in the oocyte (Fig. 2B). Lasp appears to be mildly enriched at the posterior of the oocyte and is also expressed in the pair of anterior and posterior polar follicle cells; it is also present on ring canals (Fig. 2B, data not shown). At stage 10 of oogenesis, Lasp is detected at the nurse cell borders, ring canals and around the cortex of the oocyte (Fig. 2C), and it tightly colocalizes with Oskar at the posterior pole of the oocyte [Fig. 2D-F; Fig. 5A; the inset in Fig. 2F shows a fluorescence profile of Oskar (red) and Lasp (green) peaking at similar positions across the oocyte cortex]. Similarly, co-detection of Lasp and Oskar in embryos at the preblastoderm stage shows that the proteins colocalize at the posterior pole (Fig. 3B-D). The antibody staining is specific, as no staining is detected in *lasp* mutants (Fig. 2A′, Fig. 3, Fig. 5A; see below for mutant generation). Thus, Oskar and Lasp are closely associated in both oocytes and embryos.

## *Drosophila* Lasp is an actin-binding protein

The sequence of *Drosophila* Lasp contains two NEB repeats, which are predicted to bind to actin (Chen et al., 1993). To test whether *Drosophila* Lasp binds F-actin in vitro, we expressed the N terminus of Lasp, including the LIM domain and both NEB repeats, as a Gst-fusion protein (GN) and performed co-sedimentation assays. After polymerization of purified G-actin in the presence of the GN fusion protein, GN co-sedimented with F-actin fibers (Fig. 1C). Almost no

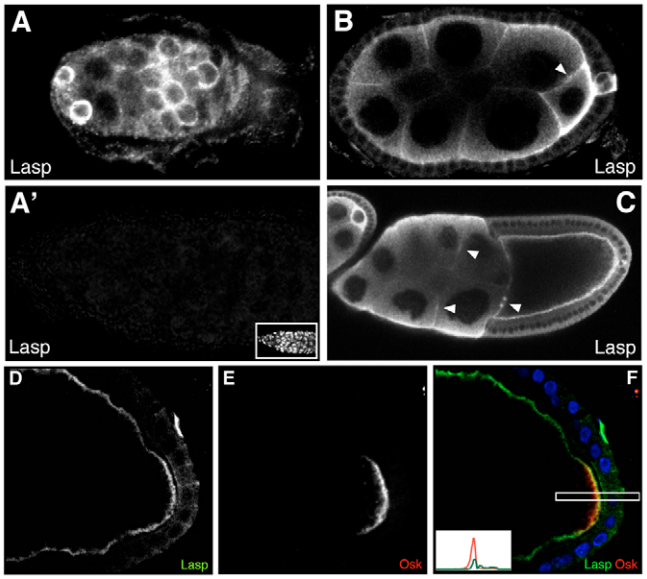


**Fig. 2. Lasp and Oskar overlap at the posterior pole of the oocyte.** (**A**) In the germarium, antibodies against Lasp strongly and specifically stain wild-type somatic cap cells and cysts in region 2, as the staining is absent in *lasp*$^{y41}$ mutants (**A′**; inset in A′ shows DAPI staining of the mutant germarium). (**B**) Stage 6 egg chamber. Lasp is strongly expressed in the nurse cells and is enriched at the posterior of the oocyte. The anterior (not in the focal plane in this image) and posterior polar follicle cells are stained as well. Lasp is mainly found around cell cortices. A stained ring canal is indicated with an arrowhead. (**C**) At stage 10, Lasp stains the periphery of nurse cells, ring canals (arrowheads) and the oocyte cortex. Weaker staining can also be detected in the follicle cells. (**D-F**) In a stage 10 oocyte, Lasp (D) and Oskar (E) colocalize at the posterior pole (F: Lasp, green; Oskar, red; DNA, blue). The inset in F shows an intensity profile across the oocyte posterior pole (region of the white square). The fluorescence intensities of both profiles peak at a similar position at the posterior cortex and demonstrate the overlapping localization.

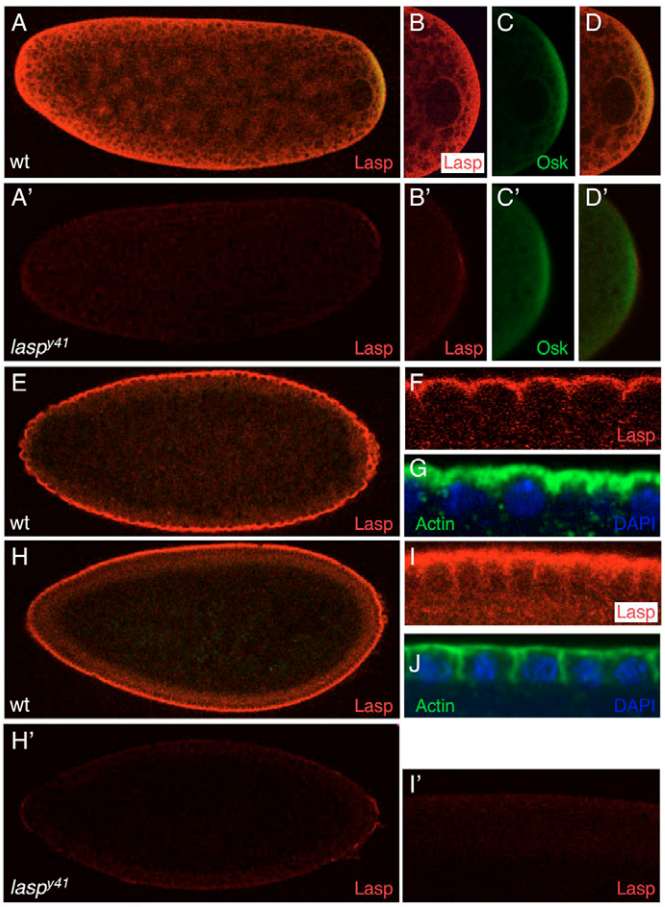


**Fig. 3. Lasp in early embryos colocalizes with Oskar and F-actin.** Confocal images of Lasp, Oskar and F-actin distribution in early embryos. (**A-D**) Lasp and Oskar overlap at the posterior pole of a wild-type preblastoderm stage embryo (A). (B-D) Magnification of the posterior tip of the embryo shown in A, stained with anti-Lasp (B) and anti-Oskar (C); merged image in D. (**A′-D′**) Corresponding stainings of a *lasp*$^{y41}$ mutant embryo. No Lasp signal is detected in the mutant, demonstrating that antibody is specific. (**E-J**) Although simultaneous detection of Lasp and F-actin was not possible for technical reasons, Lasp distribution parallels that of F-actin, extending along the network of actin fibers throughout the embryo. At the syncytial blastoderm stage, both Lasp and actin are localized apically (E-G). At the blastoderm stage, Lasp is localized apically and laterally within the epithelial cell; F-actin is distributed apically, laterally and basally (H-J). (**H′**,**I′**) Lasp staining of a *lasp*$^{y41}$ mutant blastoderm embryo, again demonstrating the specificity of the antibody.

GN protein was found in the pellet in the absence of F-actin (Fig. 1C). None of BSA, Gst alone or Gst fused to the C terminus of Lasp (lacking the NEB repeats) co-sedimented with F-actin, whereas the actin-binding protein α-actinin co-sedimented quantitatively under the same conditions (data not shown). Consistent with the antibody stainings, functional (data not shown) GFP-tagged Lasp expressed under control of the germline specific *nanos*-Gal4VP16 driver (Rorth, 1998; Van Doren et al., 1998) showed a distribution very similar to that of F-actin (Fig. 1D-F).

In the early embryo, F-actin is highly concentrated in the cortical cytoplasm as punctate aggregates and in filamentous structures (von Dassow and Schubiger, 1994). Similarly, Lasp was detected as a network throughout the embryo cytoplasm and around the cortical dense layer at the preblastoderm stage (Fig. 3A). At the syncytial blastoderm stage, Lasp accumulated apically along the invaginating plasma membrane (Fig. 3E,F), in a distribution resembling that of F-actin (Fig. 3G). At the blastoderm stage, both Lasp (Fig. 3H,I) and F-actin (Fig. 3J) accumulated apically and laterally in the epithelial cells. No Lasp staining was detected at either stage in *lasp* mutants (Fig. 3A′-D′,H′,I′). Taken together, the colocalization and binding data suggest that Lasp anchors Oskar to the actin cytoskeleton. Consistent with this hypothesis, both the cortical Lasp (see Fig. S2 in the supplementary material) and posterior Oskar localization (Babu et al., 2004) are lost upon treatment of the oocytes with the actin polymerization inhibitor Latrunculin A.

## Phenotypic characterization of *lasp* mutants

FlyBase predicts a long Lasp (L-Lasp) isoform of 660 amino acids (aa) and a short isoform of 504 aa (S-Lasp), encoded by alternatively spliced transcripts (Fig. 4A,B). The short isoform lacks a part of the spacer region encoded by the fifth exon. RT-PCR revealed that, although transcripts encoding each isoform are expressed in the ovary, only the long isoform-encoding transcript is detected in 0- to 2-hour embryos (Fig. 4C). Consistent with this,

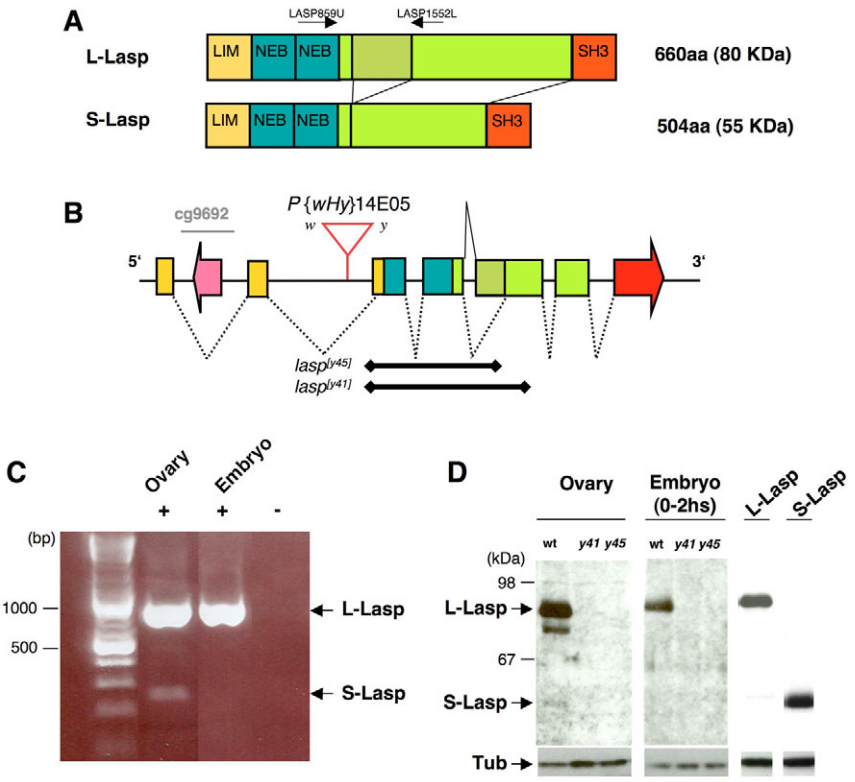


**Fig. 4. Generation and characterization of *lasp* loss-of-function mutants.** (**A**) Domain organization of *Drosophila* Lasp. S-Lasp (55 kDa) lacks sequences corresponding to the beginning of the fifth exon to 474-bp downstream of fifth exon of L-Lasp (80 kDa). (**B**) Diagram of the genomic region of *lasp*. Color code of *lasp* exons is as in A. CG9692, a predicted intronic gene (pink), is located between the first and the second exons of *lasp*. $P\{wHy\}^{DG14505}$ inserted in the second intron of *lasp* was remobilized to obtain deletions in the locus ($lasp^{y45}$ and $lasp^{y41}$; indicated by black bars). (**C**) RT-PCR on wild-type (wt) ovarian and embryonic RNA. The RT-PCR products specific for L-Lasp (upper band, 700 bp) and S-Lasp (lower band, 220 bp) were generated using the primers indicated in B. Note that a low level of the short isoform is detected in the ovary only. –, no reverse-transcriptase control. (**D**) Western analysis demonstrates the absence of Lasp in the deletion mutants $lasp^{y41}$ and $lasp^{y45}$. In the wild-type (wt) ovary extract (left panel), the antibody recognizes a major and minor band of 80 and 55 kDa corresponding to full-length L-Lasp and S-Lasp, as identified by comparison with *maternal-tubulin* driven L- and S-Lasp in a $lasp^{-}$ background (right panels). In addition, a possible degradation product of L-Lasp of 75 kDa is seen. Consistent with the RT-PCR data, in the wt embryo extract (middle panel), the antibody recognizes a single band of 80 kDa corresponding to L-Lasp. No Lasp protein is seen in the deletion mutants $lasp^{y41}$ and $lasp^{y45}$ [using antisera raised against the C terminus or N terminus (not shown)] of Lasp, confirming that they are null mutants. Tubulin was used as loading control (lower panels).

both Lasp isoforms are detected in the ovary, whereas only L-Lasp is detected in 0- to 2-hour embryos by western blotting (Fig. 4D).

To determine Lasp function during oogenesis and early embryogenesis, we generated *lasp* null alleles by remobilizing a *hobo* transposable element (Huet et al., 2002) inserted in the second intron of *lasp* ($P\{wHy\}$DG14505, kindly provided by the Gelbart laboratory, Harvard University, USA; Fig. 4B). In two of the mutants we generated, $lasp^{y41}$ and $lasp^{y45}$, a large region including exons 3, 4 and 5 of the *lasp*-coding region was deleted (Fig. 4B) and no mRNA could be detected in ovaries by RT-PCR (data not shown). Western blotting confirmed that neither S-Lasp nor L-Lasp was present in either the ovaries of $lasp^{y41}$ or $lasp^{y45}$ homozygous females, or the embryos laid by them (*lasp* mutant embryos; Fig. 4D).

$lasp^{y41}$ and $lasp^{y45}$ are semi-lethal alleles, and 40-50% of *lasp* mutant eggs fail to develop, mostly because they are unfertilized (as assessed by DAPI staining; data not shown). Hatching is restored by expressing transgenic wild-type L-Lasp, but not by expressing S-Lasp or a version of L-Lasp bearing the W→A mutation in its SH3 domain (e.g. driven by maternal *tubulin*-Gal4 or pCOG; data not shown), revealing that both the SH3 domain and the spacer region (fifth exon) are crucial for this Lasp function. The other 50-60% of embryos hatch and develop normally.

Homozygous mutant *lasp* females all contain normally developed ovaries. Oskar protein (Fig. 5A), *oskar* mRNA and Staufen protein, which is required for *oskar* mRNA localization and serves as an *oskar* mRNA reporter (data not shown) (St Johnston et al., 1991), are localized normally, and *oskar* mRNA levels appear to be normal, as evaluated by quantitative RT-PCR (data not shown). However, western blotting revealed a mild reduction in Oskar protein levels in the ovary and a strong reduction in 0- to 2-hour *lasp* mutant embryos compared with in wild-type controls (Fig. 5B). Accordingly, in situ hybridization and antibody staining of embryos derived from *lasp* mutant mothers showed reduced amounts of *oskar* RNA and protein at the posterior pole (Fig. 5C; quantification of fluorescent signals in Fig. 5D). By contrast, *bicoid* mRNA detected at the anterior pole was unchanged (Fig. 5C,D), demonstrating that the reduction was specific to *oskar*. As quantitative RT-PCR (see Fig. S3 in the supplementary material) revealed similar total levels of *oskar* mRNA in *lasp* mutant and wild-type embryos (0-2 hours), the reduced amount of localized *oskar* mRNA observed at the posterior pole of *lasp* mutant embryos did not result from mRNA degradation, but rather might result from its failure to remain localized at the posterior pole, a process that requires the Oskar protein itself (Ephrussi et al., 1991). In conclusion, *lasp* appears to be required specifically for the stable accumulation of wild-type levels of *oskar* mRNA and Oskar protein at the posterior pole of the embryo.

## Lasp promotes Oskar accumulation at the posterior pole

Oskar activity at the posterior pole is required for abdomen and germline formation in the embryo (Ephrussi et al., 1991; Lehmann and Nusslein-Volhard, 1986), with germline formation being more sensitive to reductions in Oskar dosage than is abdominal patterning and thus an ideal read-out for threshold Oskar levels (Lehmann and

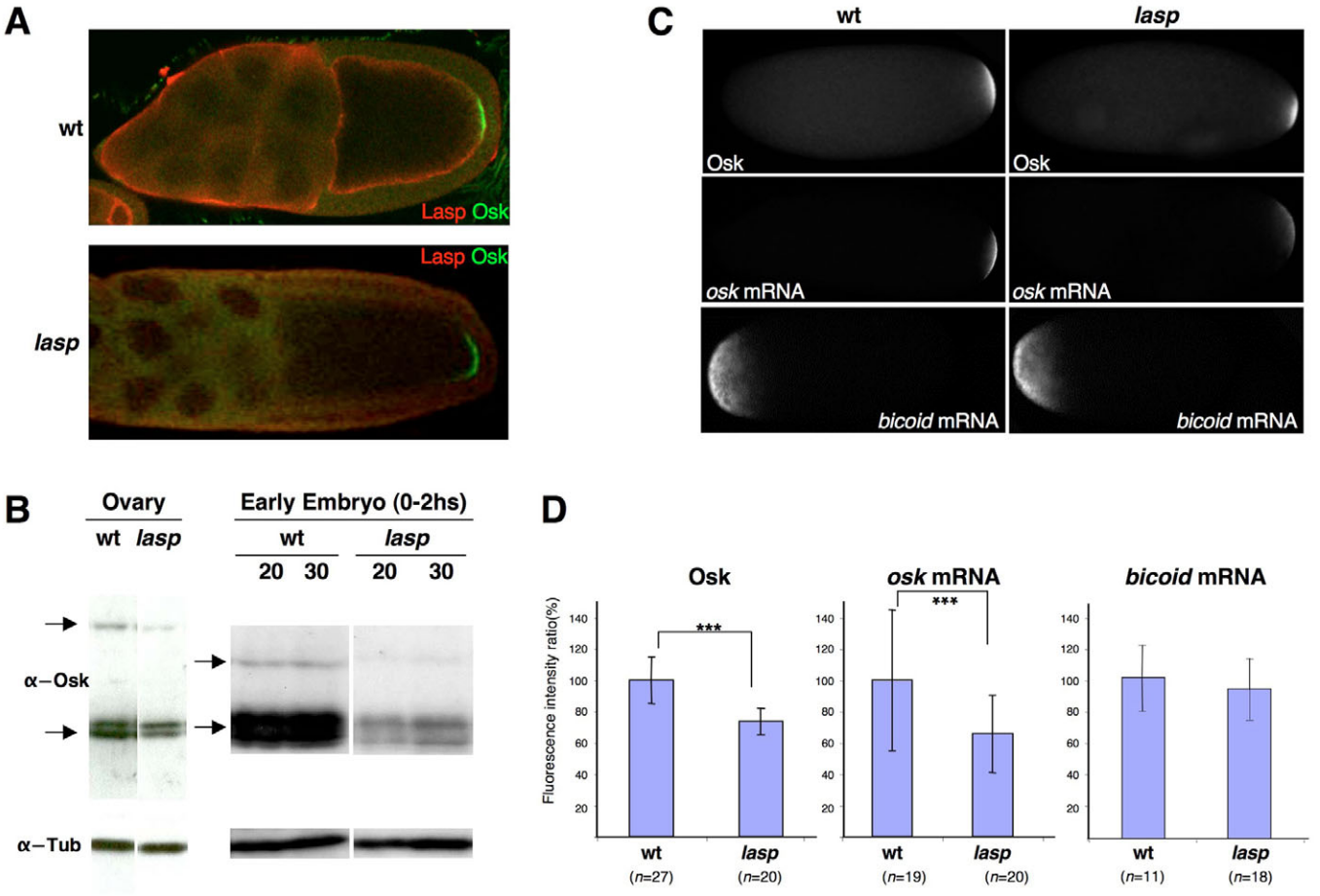


**Fig. 5. Oskar levels are reduced in *lasp* mutant embryos.** (**A**) Stage 10 wild-type (wt) and *lasp* mutant egg chambers. Lasp (red) is localized around the oocyte cortex and Oskar (green) is localized at the posterior pole (upper panel). Lasp is not detected in the *lasp* mutant, but Oskar is localized at the posterior as in wild type (lower panel). (**B**) Western blot detection of Oskar protein in extracts of wild-type and *lasp* mutant ovaries and embryos (as indicated on top of the panels). Levels of Short-Oskar as well as the N-terminal extension containing Long-Oskar (arrows) are reduced in the *lasp* mutant compared with in wild-type ovaries and embryos. α-Tubulin was used as loading control (lower panels). (**C**) Compared with *bcd* mRNA at the anterior (bottom panels), Oskar protein (top) and mRNA (middle panels) levels are reduced at the posterior of *lasp* mutant embryos. For comparison, wild-type embryos are shown on the left. (**D**) Quantification of effect shown in C. Comparison of fluorescent signal intensities showed that the reduction of Oskar protein and mRNA is specific and significant at $P<0.001$ (***).

Nusslein-Volhard, 1986). The progeny of heterozygous $osk^{54}$/+ females and $lasp^{v45}$, $osk^{54}$/+ double heterozygotes develop no germline (grandchildless phenotype) at very low frequency (e.g. $osk^{54}$/+: 1% no ovary, 8% only one ovary; Fig. 6A). By contrast, *oskar* heterozygous females lacking both copies of *lasp* show a penetrant grandchildless phenotype, with 20% of their offspring displaying a complete absence of ovaries, and another 25% having only a single ovary (Fig. 6A). Western blot analysis showed that the amount of Oskar protein in $lasp^{v45}$, $osk^{54}$/$lasp^{v45}$ ovaries was reduced by 40-50% relative to $osk^{54}$/+ ovaries (normalized to Tubulin and Kinesin Heavy Chain, respectively; see Fig. S4 in the supplementary material), which is consistent with the increased penetrance of the grandchildless phenotype.

We further quantified the effect of the absence of *lasp* in germline formation by counting the number of germ cells formed in *lasp* wild-type and mutant embryos (Fig. 6B,C). Whereas wild-type embryos displayed an average of 33 germ cells, an average of only 26 cells was observed in *lasp* mutant embryos, reflecting the reduction in Oskar levels at the posterior pole. Again, we detected a strong genetic interaction between *oskar* and *lasp*: whereas $osk^{54}$/+ embryos displayed an average of 23 germ cells, $lasp^{v45}$, $osk^{54}$/$lasp^{v45}$ embryos formed only 12.

We conclude that *oskar* and *lasp* cooperate to ensure that Oskar protein accumulates at the posterior pole of the embryo at levels that are sufficient for germline formation (see Discussion).

## An SH3 domain capable of interacting with Oskar is required for Lasp function in vivo

To test whether the SH3 domain of Lasp is required for Oskar accumulation at the posterior pole of the embryo, we performed rescue experiments using either a wild-type Lasp transgene or one bearing the W→A mutation that disrupts the Lasp-Oskar interaction in vitro (Fig. 1; see also Fig. S1 in the supplementary material). The grandchildless phenotype of $lasp^{v45}$, $osk^{54}$/$lasp^{v41}$ females was rescued almost fully by a *lasp* transgene (Fig. 7A), thereby also confirming that absence of *lasp* was responsible for the phenotype. By contrast, no rescue of the grandchildless phenotype was observed with the L-Lasp (W→A) transgene,

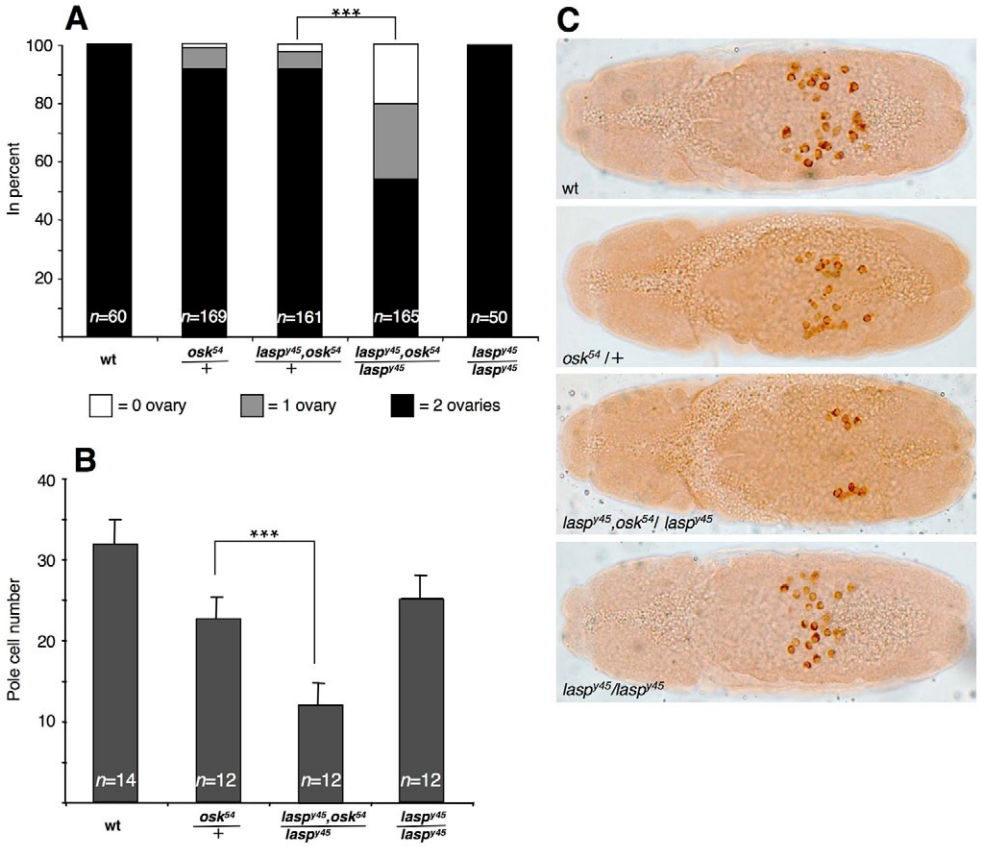


**Fig. 6. *lasp* interacts genetically with *oskar*.** (**A**) The grandchildless phenotype (absence of ovaries) was quantified by dissecting female offspring of the indicated genotypes. $lasp^{y45}$, $osk^{54}/lasp^{y45}$ females display a strong grandchildless phenotype compared with $lasp^{y45}$, $osk^{54}$/+ females (***statistically significant at $P<0.001$; $\chi^2$ test). (**B**,**C**) Pole cells of stage 11 embryos produced by females of the indicated genotypes were stained with anti-Vasa antibodies (C) and counted (B). The number of pole cells in progeny of $lasp^{y45}$, $osk^{54}/lasp^{y45}$ (12 cells on average) was half that of the $osk^{54}$/+ progeny (23 cells on average; ***$P<0.001$; two-sample *t*-test). Wild-type embryos have an average of 33 pole cells.

indicating that the SH3 domain that is crucial for the Lasp-Osk interaction in vitro is also crucial in vivo. The S-Lasp transgene also failed to rescue the phenotype. The number of germ cells detected in the progeny of $lasp^{y45}$, $osk^{54}/lasp^{y41}$ females expressing the different *lasp* transgenes (Fig. 7B,C) paralleled the penetrance of the grandchildless phenotype (Fig. 7A). These results indicate that the SH3 domain is essential for Lasp function during germline formation and that the Lasp-Oskar interaction is relevant in vivo.

## Lasp controls Oskar accumulation at the cortex of the embryo

It has been shown that wild-type Oskar protein produced from an *oskar-K103′UTR* transgene accumulates around the entire oocyte cortex (Riechmann et al., 2002; Vanzo and Ephrussi, 2002). Consequently, the embryos develop anterior patterning defects or even a bicaudal phenotype, in which anterior structures (head and thorax) are replaced by a duplicated abdomen of reversed polarity (Fig. 8A). To test whether Lasp is required for this ectopic Oskar-induced phenotype, we expressed the *osk-K103′UTR* transgene in *lasp* mutant females. Indeed, whereas wild-type females expressing the *osk-K103′UTR* transgene produced embryos that displayed the full range of Oskar-related anterior patterning phenotypes with high penetrance, embryos of *lasp* mutant *osk-K103′UTR* females showed anterior patterning defects with both significantly reduced penetrance and severity (Fig. 8A,B).

Similarly, an *oskar-bicoid* (*osk-bcd*) 3′UTR transgene (Ephrussi and Lehmann, 1992) caused the formation of ectopic pole cells at the anterior in 43% of embryos, whereas in a *lasp* mutant background, pole cells formed at the anterior in only 10% of embryos (Fig. 8C). Furthermore, only 20% of the embryos of $lasp^{y41}$/+ females developed pole cells at the anterior pole, revealing an effect of *lasp* gene dosage on Oskar accumulation. All fertilized eggs produced by *osk-bcd*-expressing $lasp^{y41}$ females developed into embryos displaying the bicaudal phenotype, confirming that abdominal patterning is less sensitive than germ cell formation to the reduction of Oskar levels in the embryo. Taken together, these results demonstrate that Lasp is necessary to achieve the high levels of Oskar activity required for pole cell formation in the embryo.

## DISCUSSION

We have shown that the *Drosophila* homolog of mammalian Lasp1 interacts via its SH3 domain with Oskar, binds directly to F-actin in vitro, and colocalizes with F-actin in vivo. Western analysis of *lasp* mutant oocytes shows a slight reduction in Oskar levels that is not readily visualized by in situ hybridization. Posterior *oskar* mRNA maintenance in the ovary, which depends on Oskar protein, also appears to be relatively normal. However, in the embryos laid by *lasp* mutant mothers (*lasp* mutant embryos), *oskar* protein and mRNA at the posterior pole are strongly reduced. The overlap of Oskar, Lasp and actin distributions at the posterior pole during oogenesis and early embryogenesis (Figs 2, 3; Fig. 5A), as well as the actin- and Oskar-binding properties of Lasp (Fig. 1), suggest that Lasp connects Oskar to actin. This is further supported by the genetic interaction between *oskar* and *lasp*, and the dependence of ectopic Oskar activity on Lasp. We therefore propose that Lasp links Oskar to the actin cytoskeleton and helps to restrict Oskar activity to the posterior pole after its localized translation. Even though we cannot exclude that Lasp also protects Oskar from degradation, the reduced amounts of *oskar* mRNA and Oskar protein observed in *lasp* mutants are probably due to the interdependence of *oskar*

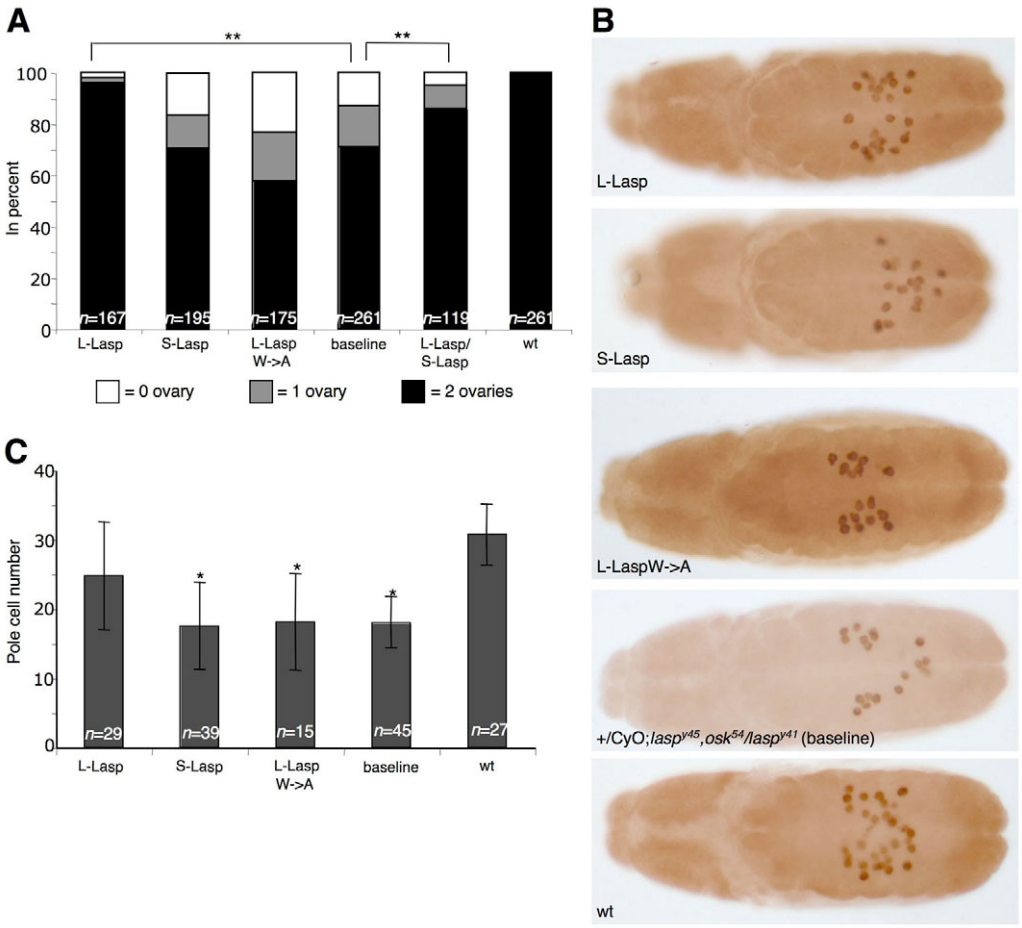


**Fig. 7. The Lasp SH3 domain is required for Lasp-Oskar interaction in vivo.** (**A**) pCOG driven L-Lasp rescues the grandchildless phenotype of $lasp^{y45}$, $osk^{54}/lasp^{y41}$ females (+/*Cyo*; $lasp^{y45}$, $osk^{54}/lasp^{y41}$, baseline; $^{**}P<0.01$; $\chi^2$ test). Neither the non-Oskar-binding SH3 variant of L-Lasp (L-LaspW→A) nor S-Lasp was able to rescue the grandchildless phenotype, suggesting an essential role for the Lasp-Oskar interaction in vivo. (**B**,**C**) Examples of stage 11 embryos laid by mothers of the indicated genotypes stained with anti-Vasa antibodies to visualize the pole cells (B). The reduced pole cell number of $lasp^{y45}$, $osk^{54}/lasp^{y41}$ embryos was partially rescued by pCOG L-Lasp (C; 25 cells on average; $^{*}P<0.05$; two-sample *t*-test), but not by pCOG L-Lasp (W→A) nor pCOG S-Lasp, again suggesting an in vivo relevance of a direct Oskar-Lasp interaction. Similar results were obtained using UAS-Lasp transgenes driven by maternal *tubulin*-Gal4VP16 or pCOG Gal4Vp16 (data not shown).

mRNA localization and Oskar protein. Less well-anchored Oskar cannot keep its mRNA restricted to the posterior pole, which in turn leads to less mRNA available for localized translation.

Lasp concentrates in actin-rich subcellular regions, including focal adhesions and lamellipodia in migrating cells (Butt et al., 2003; Chew et al., 2002; Schreiber et al., 1998; Terasaki et al., 2004), and motile growth cones of cultured neurons (Phillips et al., 2004). In our study, we have shown that the NEB repeats of *Drosophila* Lasp bind actin in vitro and that Lasp colocalizes with actin in vivo. *lasp* mutant egg-chambers display no obvious actin defects, consistent with the observation that rabbit Lasp1 has no detectable effect on actin polymerization and that cells depleted of Lasp1 can form focal adhesions (Chew et al., 2002; Chew et al., 2000). Lasp1 has also been shown to be a substrate of protein kinase A (PKA) (Chew et al., 1998; Schreiber et al., 1998). After PKA stimulation of parietal cells in isolated gastric glands, Lasp1 redistributes from cortical regions to the actin-rich intracellular canalicular region (Chew et al., 2000). In *Drosophila*, egg chambers lacking PKA catalytic subunit activity contain multinucleate nurse cells and abnormal ring canals. In addition, *pka* mutant oocytes fail to respond to a signal from posterior follicle cells and consequently fail to reorganize the microtubule cytoskeleton (Lane and Kalderon, 1993; Lane and Kalderon, 1994). Oocytes lacking Lasp function show neither of these phenotypes. By contrast, excess PKA activity, as in *Pka-RI* mutant oocytes, causes the accumulation of high levels of ectopic Oskar protein and embryos displaying the bicaudal phenotype (Yoshida et al., 2004). This ectopic accumulation could be due to de-localized *oskar* mRNA translation, or to the stabilization of Oskar protein produced ectopically that would normally be targeted for degradation. Given the reduced Oskar levels we observed in *lasp* mutant embryos and the dependence of ectopic Oskar activity on Lasp (Figs 7, 8), it would be interesting to determine whether PKA phosphorylation of Lasp contributes either to the accumulation of Oskar or to its anchoring in the embryo.

Oskar anchoring becomes crucial at stage 10B of oogenesis, when cytoplasmic streaming starts, a vigorous process that ensures the mixing and even distribution of cytoplasmic mRNAs and proteins in the egg (Gutzeit and Koppa, 1982). Treatment of embryos with the actin-severing drugs Cytochalasin D and Latrunculin A disrupts the localization of *oskar* mRNA and protein, but not of *bicoid* mRNA (Lantz et al., 1999), which is similar to what we observed in *lasp* mutant embryos and consistent with a role of Lasp in actin-

**A**

| | | wt (*n*=190) | *osk-K10* ; +/+ (*n* = 2122) | *osk-K10* ;*lasp*$^{y41}$/*lasp* $^{y41}$ (*n* = 833) | *lasp*$^{y41}$/*lasp* $^{y41}$ (*n*= 124 ) |
|---|---|---|---|---|---|
| Hatched: | | 88.3 | 27.3 | 46.6 | 55.6 |
| Unhatched: | Unfertilized: | 11.7 | 10.8 | 33.5 | 44.4 |
| | Head defect: | 0 | 4.2 | 6.4 | 0 |
| | Weak bicaudal: | 0 | 29.9 | 13.3 | 0 |
| | Strong bicaudal: | 0 | 11.0 | 0.2 | 0 |
| | Shapeless: | 0 | 16.4 | 0 | 0 |

**B**

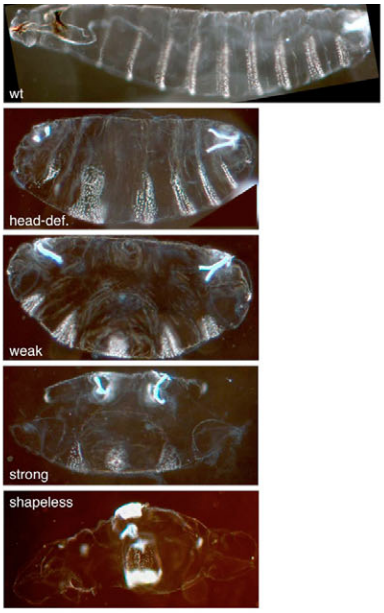


**C**

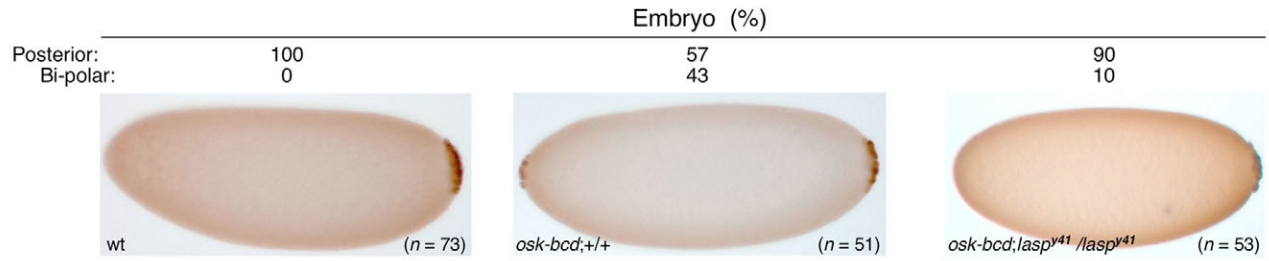


**Fig. 8. Lasp regulates tight localization of Oskar in the embryo.** (**A**) Hatch rate of embryos and cuticle analysis of unhatched embryos with defects produced by wild-type (wt) or *lasp* mutant females expressing the osk-*K10* 3′UTR transgene under maternal *tubulin*-Gal4 control. Removal of *lasp* reduces the phenotype of ectopic Oskar. (**B**) Representative cuticle examples of – top to bottom – wild-type, head-defect, mild and strong bicaudal and shapeless classes of defects scored in A. (**C**) Pole cell staining of cellular blastoderm-stage embryos laid by wild-type or *lasp* mutant females, respectively, expressing the *osk-bcd* 3′UTR as indicated. Pole cells are stained with anti-Vasa antibody. The removal of *lasp* reduces the percentage of embryos with ectopic, anterior pole cells (as indicated above each panel).

dependent Oskar anchoring. Several mechanisms contribute to *oskar* RNA and protein anchoring. Bifocal (Bif) and Homer (Hom) redundantly promote Oskar anchoring at the oocyte posterior pole via an actin-dependent and an unknown, actin-independent process, respectively (Babu et al., 2004). Remarkably, the Oskar detachment defects of Latrunculin A-treated *hom* egg chambers are stronger than in *hom/bif* double mutants (Babu et al., 2004), suggesting there are additional actin-dependent attachment mechanisms. However, we were unable to detect genetic interactions between *lasp* and *hom/bif*, as neither *hom/lasp* nor *bif/lasp* double mutants showed an Oskar localization defect in ovaries (data not shown).

The ubiquitous expression of Oskar in the oocyte leads to its enrichment all around the cortex, indicating that Oskar protein can be recruited all around the F-actin-rich oocyte cortex (data not shown) (Riechmann et al., 2002). As Lasp is uniformly distributed along the actin-rich cortex, it could participate in Oskar anchoring at ectopic cortical locations. Consistent with this, the deleterious effects of ectopic anterior (*osk-bcd*) or cortical (*osk-K10*) Oskar on embryonic patterning are suppressed in *lasp* mutant embryos. In further support of our anchoring model, only Lasp with a functional SH3 domain (i.e. one capable of interacting with Oskar in vitro and in the two-hybrid assay; see Fig. 1 and below; see also Fig. S1 in the supplementary material), is able to rescue the grandchildless phenotype and the reduction in pole cell number observed in *osk*$^{-}$, *lasp*$^{-}$/*lasp*$^{-}$ embryos.

The interaction of Oskar with Lasp depends on its SH3 domain, because a single W→A point mutation on the binding surface of the SH3 domain abolishes its binding to Oskar (Fig. 1; see also Fig. S1 in the supplementary material). SH3 domains usually interact with short, proline-rich sequences with the consensus RxxPxxP (class I binding site) or PxxPxR (class II binding site) (Kay et al., 2000). The region of Oskar that is sufficient to interact with the SH3 domain of Lasp (aa 290-369; data not shown) does not encode a perfect class I or class II binding site, nor does it contain any of the less frequently occurring SH3-binding motifs (Kang et al., 2000; Mongiovi et al., 1999). Three PxxP motifs are present within the SH3-binding region of Oskar, but all of them lack the neighboring basic amino acid. Nevertheless, Oskar is highly specific for the SH3 domain of Lasp, as it does not interact with six other SH3 domains tested, and the interaction capability is conserved in Oskar of *D. virilis* (not shown).

Interestingly, the Lasp SH3 domain shares a high degree of similarity with several proteins involved in clathrin-mediated endocytosis: the actin-binding proteins Cortactin and Abp1, as well as Syndapin and Amphiphysin, both of which bind Dynamin and

contain an F-actin- or an Arp2/3-interacting domain (Qualmann and Kessels, 2002). It has been reported that both Lasp and Dynamin II localize to the apical membrane of parietal cells, and that they interact in vitro (Okamoto et al., 2002). Thus, it is possible that Lasp is not only an actin binding-protein, but is also involved in vesicle trafficking. Endocytic trafficking and actin-based mechanisms also contribute to Oskar anchoring, and it is thus possible that Lasp, together with other functionally related proteins, represents a link between these processes. Furthermore, one of the two Oskar isoforms – Long-Oskar – plays a crucial role in the anchoring of both Oskar isoforms and *oskar* mRNA at the oocyte cortex at stage 10 of oogenesis (Vanzo and Ephrussi, 2002). Oocytes lacking Oskar have a dramatically reduced endocytic compartment and lack the thick actin bundles that are normally observed at the posterior pole. Thus Oskar anchoring in the oocyte appears to be a dynamic process, with Oskar-stimulated recycling endocytosis and filamentous actin outgrowths playing an important role in the maintenance of Oskar at the cell cortex (Tanaka and Nakamura, 2008; Vanzo et al., 2007). It is thus conceivable that Oskar, Lasp, and other possibly redundant actin-binding proteins act in feedback loops with components of the endocytic pathway to maintain Oskar at the posterior pole.

We are grateful to E. A. Golemis, G. Superti-Furga, P. Rørth, I. Reckmann, M. Way, J. Ellenberg, J. Wittbrodt, D. St Johnston and A. F. Straight for help, advice, antibodies and constructs. We thank J. Grosshans and C. Nüsslein-Volhard, A. Spradling and the BDGP for libraries, and H. D. Lipshitz and the Developmental Studies Hybridoma Bank for antibodies. We thank the EMBL Genomics Core Facility and Elisa Wurmbach for sequencing and Q/RT-PCR analysis, T. Zimmerman (EMBL-ALMF) for advice on quantifications, EMBL Laboratory Animal Resources for the generation of antibodies, and S. Castagnetti, V. Riechmann, S. Yoshida, E. Wurmbach, J. Curtiss, F. Besse and Anne Muesch for critically reading the manuscript. S.C. was supported by a fellowship from the Fundação para a Ciência e a Tecnologia, Portugal, and A.J. by an EMBO fellowship and an HFSPO grant to A.E.

**Supplementary material**

Supplementary material for this article is available at http://dev.biologists.org/cgi/content/full/136/1/95/DC1

**References**

**Babu, K., Cai, Y., Bahri, S., Yang, X. and Chia, W.** (2004). Roles of Bifocal, Homer, and F-actin in anchoring Oskar to the posterior cortex of Drosophila oocytes. *Genes Dev.* **18**, 138-143.

**Breitwieser, W., Markussen, F. H., Horstmann, H. and Ephrussi, A.** (1996). Oskar protein interaction with Vasa represents an essential step in polar granule assembly. *Genes Dev.* **10**, 2179-2188.

**Butt, E., Gambaryan, S., Gottfert, N., Galler, A., Marcus, K. and Meyer, H. E.** (2003). Actin binding of human LIM and SH3 protein (LASP) is regulated by cGMP- and cAMP-dependent protein kinase phosphorylation on Ser-146. *J. Biol. Chem.* **278**, 15601-15607.

**Chen, M. J., Shih, C. L. and Wang, K.** (1993). Nebulin as an actin zipper: a two-module nebulin fragment promotes actin nucleation and stabilizes actin filaments. *J. Biol. Chem.* **268**, 20327-20334.

**Chew, C. S., Parente, J. A., Zhou, C., Baranco, E. and Chen, X.** (1998). Lasp-1 is a regulated phosphoprotein within the cAMP signaling pathway in the gastric parietal cell. *Am. J. Physiol.* **275**, C56-C67.

**Chew, C. S., Parente, J. A., Chen, X., Chaponnier, C. and Cameron, R. S.** (2000). The LIM and SH3 domain-containing protein, lasp-1, may link the cAMP signaling pathway with dynamic membrane restructuring activities in ion transporting epithelia. *J. Cell Sci.* **113**, 2035-2045.

**Chew, C. S., Chen, X., Parente, J. A., Jr, Tarrer, S., Okamoto, C. and Qin, H. Y.** (2002). Lasp-1 binds to non-muscle F-actin *in vitro* and is localized within multiple sites of dynamic actin assembly *in vivo*. *J. Cell Sci.* **115**, 4787-4799.

**Driever, W. and Nusslein-Volhard, C.** (1988). A gradient of bicoid protein in Drosophila embryos. *Cell* **54**, 83-93.

**Ephrussi, A. and Lehmann, R.** (1992). Induction of germ cell formation by oskar. *Nature* **358**, 387-392.

**Ephrussi, A., Dickinson, L. K. and Lehmann, R.** (1991). Oskar organizes the germ plasm and directs localization of the posterior determinant nanos. *Cell* **66**, 37-50.

**Fromont-Racine, M., Rain, J. C. and Legrain, P.** (1997). Toward a functional analysis of the yeast genome through exhaustive two-hybrid screens. *Nat. Genet.* **16**, 277-282.

**Grosshans, J., Schnorrer, F. and Nusslein-Volhard, C.** (1999). Oligomerisation of Tube and Pelle leads to nuclear localisation of dorsal. *Mech. Dev.* **81**, 127-138.

**Grunewald, T. G. and Butt, E.** (2008). The LIM and SH3 domain protein family: structural proteins or signal transducers or both? *Mol. Cancer* **7**, 31.

**Gutzeit, H. O. and Koppa, R.** (1982). Time-lapse film analysis of cytoplasmic streaming during late oogenesis of *Drosophila*. *J. Embryol. Exp. Morphol.* **67**, 101-111.

**Hachet, O. and Ephrussi, A.** (2004). Splicing of oskar RNA in the nucleus is coupled to its cytoplasmic localization. *Nature* **428**, 959-963.

**Huet, F., Lu, J. T., Myrick, K. V., Baugh, L. R., Crosby, M. A. and Gelbart, W. M.** (2002). A deletion-generator compound element allows deletion saturation analysis for genomewide phenotypic annotation. *Proc. Natl. Acad. Sci. USA* **99**, 9948-9953.

**Kang, H., Freund, C., Duke-Cohan, J. S., Musacchio, A., Wagner, G. and Rudd, C. E.** (2000). SH3 domain recognition of a proline-independent tyrosine-based RKxxYxxY motif in immune cell adaptor SKAP55. *EMBO J.* **19**, 2889-2899.

**Kay, B. K., Williamson, M. P. and Sudol, M.** (2000). The importance of being proline: the interaction of proline-rich motifs in signaling proteins with their cognate domains. *FASEB J.* **14**, 231-241.

**Kim-Ha, J., Smith, J. L. and Macdonald, P. M.** (1991). oskar mRNA is localized to the posterior pole of the Drosophila oocyte. *Cell* **66**, 23-35.

**Kim-Ha, J., Kerr, K. and Macdonald, P. M.** (1995). Translational regulation of oskar mRNA by bruno, an ovarian RNA-binding protein, is essential. *Cell* **81**, 403-412.

**Labeit, S. and Kolmerer, B.** (1995). The complete primary structure of human nebulin and its correlation to muscle structure. *J. Mol. Biol.* **248**, 308-315.

**Lane, M. E. and Kalderon, D.** (1993). Genetic investigation of cAMP-dependent protein kinase function in Drosophila development. *Genes Dev.* **7**, 1229-1243.

**Lane, M. E. and Kalderon, D.** (1994). RNA localization along the anteroposterior axis of the Drosophila oocyte requires PKA-mediated signal transduction to direct normal microtubule organization. *Genes Dev.* **8**, 2986-2995.

**Lantz, V. A., Clemens, S. E. and Miller, K. G.** (1999). The actin cytoskeleton is required for maintenance of posterior pole plasm components in the Drosophila embryo. *Mech. Dev.* **85**, 111-122.

**Lehmann, R. and Nusslein-Volhard, C.** (1986). Abdominal segmentation, pole cell formation, and embryonic polarity require the localized activity of oskar, a maternal gene in Drosophila. *Cell* **47**, 141-152.

**Lin, H., Yue, L. and Spradling, A. C.** (1994). The *Drosophila* fusome, a germline-specific organelle, contains membrane skeletal proteins and functions in cyst formation. *Development* **120**, 947-956.

**Lock, P., Fumagalli, S., Polakis, P., McCormick, F. and Courtneidge, S. A.** (1996). The human p62 cDNA encodes Sam68 and not the RasGAP-associated p62 protein. *Cell* **84**, 23-24.

**Markussen, F. H., Michon, A. M., Breitwieser, W. and Ephrussi, A.** (1995). Translational control of oskar generates short OSK, the isoform that induces pole plasma assembly. *Development* **121**, 3723-3732.

**Mongiovi, A. M., Romano, P. R., Panni, S., Mendoza, M., Wong, W. T., Musacchio, A., Cesareni, G. and Di Fiore, P. P.** (1999). A novel peptide-SH3 interaction. *EMBO J.* **18**, 5300-5309.

**Musacchio, A., Gibson, T., Lehto, V. P. and Saraste, M.** (1992a). SH3-an abundant protein domain in search of a function. *FEBS Lett.* **307**, 55-61.

**Musacchio, A., Noble, M., Pauptit, R., Wierenga, R. and Saraste, M.** (1992b). Crystal structure of a Src-homology 3 (SH3) domain. *Nature* **359**, 851-855.

**Musacchio, A., Saraste, M. and Wilmanns, M.** (1994). High-resolution crystal structures of tyrosine kinase SH3 domains complexed with proline-rich peptides. *Nat. Struct. Biol.* **1**, 546-551.

**Okamoto, C. T., Li, R., Zhang, Z., Jeng, Y. Y. and Chew, C. S.** (2002). Regulation of protein and vesicle trafficking at the apical membrane of epithelial cells. *J. Control Release* **78**, 35-41.

**Phillips, G. R., Anderson, T. R., Florens, L., Gudas, C., Magda, G., Yates, J. R., 3rd and Colman, D. R.** (2004). Actin-binding proteins in a postsynaptic preparation: Lasp-1 is a component of central nervous system synapses and dendritic spines. *J. Neurosci. Res.* **78**, 38-48.

**Qualmann, B. and Kessels, M. M.** (2002). Endocytosis and the cytoskeleton. *Int. Rev. Cytol.* **220**, 93-144.

**Riechmann, V. and Ephrussi, A.** (2004). Par-1 regulates bicoid mRNA localisation by phosphorylating Exuperantia. *Development* **131**, 5897-5907.

**Riechmann, V., Gutierrez, G. J., Filardo, P., Nebreda, A. R. and Ephrussi, A.** (2002). Par-1 regulates stability of the posterior determinant Oskar by phosphorylation. *Nat. Cell Biol.* **4**, 337-342.

**Rongo, C., Gavis, E. R. and Lehmann, R.** (1995). Localization of oskar RNA regulates oskar translation and requires Oskar protein. *Development* **121**, 2737-2746.

**Rorth, P.** (1998). Gal4 in the Drosophila female germline. *Mech. Dev.* **78**, 113-118.

**Rubin, G. M. and Spradling, A. C.** (1982). Genetic transformation of Drosophila with transposable element vectors. *Science* **218**, 348-353.

**Schreiber, V., Moog-Lutz, C., Regnier, C. H., Chenard, M. P., Boeuf, H., Vonesch, J. L., Tomasetto, C. and Rio, M. C.** (1998). Lasp-1, a novel type of actin-binding protein accumulating in cell membrane extensions. *Mol. Med.* **4**, 675-687.

**St Johnston, D., Beuchle, D. and Nusslein-Volhard, C.** (1991). Staufen, a gene required to localize maternal RNAs in the Drosophila egg. *Cell* **66**, 51-63.

**Tanaka, T. and Nakamura, A.** (2008). The endocytic pathway acts downstream of Oskar in Drosophila germ plasm assembly. *Development* **135**, 1107-1117.

**Terasaki, A. G., Suzuki, H., Nishioka, T., Matsuzawa, E., Katsuki, M., Nakagawa, H., Miyamoto, S. and Ohashi, K.** (2004). A novel LIM and SH3 protein (lasp-2) highly expressing in chicken brain. *Biochem. Biophys. Res. Commun.* **313**, 48-54.

**Tomancak, P., Piano, F., Riechmann, V., Gunsalus, K. C., Kemphues, K. J. and Ephrussi, A.** (2000). A Drosophila melanogaster homologue of Caenorhabditis elegans par-1 acts at an early step in embryonic-axis formation. *Nat. Cell Biol.* **2**, 458-460.

**Van Doren, M., Williamson, A. L. and Lehmann, R.** (1998). Regulation of zygotic gene expression in Drosophila primordial germ cells. *Curr. Biol.* **8**, 243-246.

**Vanzo, N. F. and Ephrussi, A.** (2002). Oskar anchoring restricts pole plasm formation to the posterior of the Drosophila oocyte. *Development* **129**, 3705-3714.

**Vanzo, N., Oprins, A., Xanthakis, D., Ephrussi, A. and Rabouille, C.** (2007). Stimulation of endocytosis and actin dynamics by Oskar polarizes the Drosophila oocyte. *Dev. Cell* **12**, 543-555.

**von Dassow, G. and Schubiger, G.** (1994). How an actin network might cause fountain streaming and nuclear migration in the syncytial Drosophila embryo. *J. Cell Biol.* **127**, 1637-1653.

**Yoshida, S., Muller, H. A., Wodarz, A. and Ephrussi, A.** (2004). PKA-R1 spatially restricts Oskar expression for Drosophila embryonic patterning. *Development* **131**, 1401-1410.